Aalborg Universitet

AALBORG UNIVERSITY

Hybrid Control of a Two-Wheeled Automatic-Balancing Robot with Backlash Feature

Durdevic, Petar; Yang, Zhenyu

Hybrid Control of a Two-Wheeled Automatic-Balancing Robot with Backlash Feature

Petar Durdevic

Department of Energy Technology
Aalborg University, Esbjerg Campus
Niels Bohrs Vej 8, 6700 Esbjerg, Denmark
Email: ploehn08@student.aau.dk

Zhenyu Yang

Department of Energy Technology
Aalborg University, Esbjerg Campus
Niels Bohrs Vej 8, 6700 Esbjerg, Denmark
Email: yang@et.aau.dk

Abstract—**This paper investigates the application of hybrid control for an automatic balancing robot system subject to backlash effect. The developed controller is a type of sliding mode controller, refereed to as a switching controller, with respect to different situations i.e., whether the backlash is present in the system operation or not. The switching controller is further weighted by a tilt angle dependent weighting function, in order to enforce the linear controller at higher angles. The proposed solution is implemented and tested on a custom developed robot platform. The extensive tests and comparisons with other solutions show the proposed solution can lead to a very satisfactory anti-backlash performance, with an easy and cost-effective implementation.**

NOMENCLATURE

Name		Unit	Constants	
v_a	=	Voltage over the armature $[V]$		
m_p	=	Body mass $[Kg]$	=	2.150
L_a	=	Motor inductance $[mH]$	=	4.658
R_a	=	Motor resistance $[\Omega]$	=	3.45
K_e	=	Back EMF constant $[sec/rad]$	=	0.026
K_t	=	Motor torque constant $[Nm/A]$	=	0.026
b	=	Viscous friction $[Nm]$	=	0.0000226
l_g	=	Distance from the pivot to the gravitational center $[m]$	=	0.06
J_w	=	Moment of inertia of the wheel $[Kg \cdot m^2]$	=	0.000057
J_p	=	Moment of inertia of the pendulum $[Kg \cdot m^2]$	=	0.211527
J_m	=	Moment of inertia of the motor shaft $[Kg \cdot m^2]$	=	0.001401
r_w	=	Wheel radius $[m]$	=	0.1
m_w	=	Mass of the wheel $[kg]$	=	0.055
2α	=	The double backlash angle $[rad]$	=	0.366
k_s	=	Shaft elasticity $[Nm/rad]$		
c_s	=	Inner damping coefficient of the shaft $[Nm/(rad/s)]$		
T_s	=	Shaft torque $[Nm]$		
T_m	=	Motor torque $[Nm]$		
T_d	=	Load torque $[Nm]$		
Θ_l	=	Load angle $[rad]$		
Θ_m	=	Motor angle $[rad]$		
Θ_s	=	Angle of the shaft on the load side $[rad]$		
Θ_g	=	Angle of the shaft on the gear side $[rad]$		
J_l	=	Load moment of Inertia $[kg \cdot m^2]$		
Θ_d	=	$\Theta_m/G_r - \Theta_l$ The total shaft displacement.		
Θ_b	=	$\Theta_d - \Theta_s$ The backlash angle represented as the difference between the total shaft displacement angle and the shaft angle.		
G_r	=	Gearing ratio		
i_a	=	Current through the armature $[A]$		
τ_w	=	Wheel torque $[A]$		
$F_p H$	=	Horizontal force created by the pendulum $[N]$		
C_b	=	Weight for the weighting controller		
$f(\Theta_p)$	=	Pendulum angle dependent weighting function $[\Theta_p \cdot C_w]$		
C_w	=	Tuning parameter of the backlash control		
M_b	=	Backlash critical angle		
H_b	=	Less critical backlash angle		

I. INTRODUCTION

Backlash is a common phenomenon for many mechanical systems with gear transmission. The backlash severity depends on the gaps between gear teeth. This work uses a multi-layer gear transmission system where the multiple bearings and gear teeth represent the backlash in the system. Nevertheless, a good design of a gear transmission system often needs to balance the teeth's gap ranges with the induced friction to the transmission system [5], [7], [9].

If the backlash effect is not carefully handled, there is a huge risk that the system may conduct a poor performance in a manner consisting of high frequency oscillations, or even turn to be unstable which can lead to an unsafe system for the operator [6]. The backlash problem can also make the stabilization of an open-loop unstable system more challenging [5]. Moreover, the backlash effect also increases the risk of wear and tear in the gears and other sensitive parts of the considered system. This can shorten the component's lifetime and increase the failure rates [6].

There are two general ways to cope with the backlash problem, if it needs to be taken care of: one way is to choose a well designed gear transmission system; alternatively, some special control strategy needs to be deployed once the backslash phenomenon appears [14]. The first solution is hardware based and can easily be adopted, for example, to use expensive zero backlash motors, but this type of solution may cause an economic concern. The second type of solution is software based and thereby very cost-effective, however, it often requires a more sophisticated control strategy than just standard PID or linear control solutions [5].

Backlash effect modeling and control has been extensively studied in recent decades. Some typical methods can be found in the survey papers [5], [6] and references therein. From a control point of view, the backlash effect could be mitigated using some specific adaptive control [2], dedicated torque compensation [9], switching control [11] or dedicated non-linear control method [12] etc.. There is no doubt that designing a controller which copes with the backlash enables saving resources, by enabling the use of cheaper motors and gearing which tend to suffer from more backlash than expensive motors.

The aim of this work is not to propose some new theoretical model or breakthrough control method for handling backlash effect, instead, this work focuses on the application

of hybrid (switching) control to handle the backslash problem on a two-wheeled automatic balancing robot system. The development of standard controllers, different mode controllers and weighted switches are discussed, implemented and tested on a developed mini Segway-type of robot system. The developed control solution is relatively simple and very easy to implement, along with quite satisfactory performance and robustness. The idea proposed here requires the estimated backlash angle, which is achieved by tracking the position of the motor [13].

The rest of the paper is organized as the following: Section II introduces the considered robot system platform; Section III proposes a set of mathematical models of the concerned robot system, including the non-linear and linear models; Section IV discusses the hybrid switching control design, Section V illustrates some testing results; and finally, we conclude the paper in Section VI.

II. CONSIDERED ROBOT PLATFORM

For this work a custom body is built, the objective of the platform is to realize an automatically self-balancing robot system, like the Segway principle. The platform holds two geared DC motors (MicroMotors - E 192), which are supplied with a 12 volt 2.2 A Lithium Ion battery, controlled by a PWM signal generated by a micro controller (PIC32MX795F512) and amplified by two H-bridges (VNH2SP30). The gear ratio is 1:18 and the backlash is measured to $\approx 1.3°$ on the geared side and $\approx 22°$ on the motor side. The micro controller is an 80 MIPS 32 bit MCU, with 10 bit ADC and 8 bit PWM. The navigational sensors are an accelerometer (ADXL345), a gyroscope (ITG-3200) and an encoder (AM512BD01). The advantage of this platform, is that it is light, which is causing the gearing to suffer badly from backlash effect. A photo of this self-developed robot is illustrated in Figure 1.
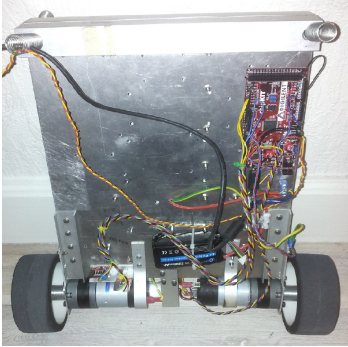

Fig. 1.   Photo of the self-developed platform.

III. MATHEMATICAL MODELING

A. Linear Model

By using the physical modeling principle, a linear model of the considered robot system is obtained in Equation 1, without taking the backlash issue into consideration at this moment.

$$\begin{cases} J_m\ddot{\Theta}_m & = K_t\frac{v_a - K_e\dot{\Theta}_m}{R_a} - b\dot{\Theta}_m - \tau_w \\ \tau_w & = J_w\ddot{\Theta}_w - F_pH \cdot r_w + m_w\ddot{\Theta}_w r_w{}^2 \\ \ddot{\Theta}_w & = \frac{J_p\ddot{\Theta}_p + m_p l_g{}^2\ddot{\Theta}_p}{-m_p r_w l_g} \end{cases} \quad (1)$$

The motor produces a torque when supplied with a voltage, this torque turns the rotor which is connected to the wheels. The wheels act as a parasitic torque τ_w on the motor [11], as they are effected by the friction of the ground f_r as illustrated in the left diagram of Figure 2. The motor armature is connected rigidly to the robot body. If the body angle gets over $0°$, the robot will be affected by the gravity which pulls the rigid body down at the centre of gravity c_g. This movement creates a horizontal force F_pH at the pivot where it is calculated accordingly $F_pH = m_p \cdot \vec{a}_{x,g}$. The gravitational acceleration in the horizontal axis $\vec{a}_{x,g}$ is found by the kinematic Equation:

$$\vec{r} = \vec{x}i + \vec{y}j \rightarrow \vec{a}_{x,g} = \vec{a}_{x,P} + \vec{a}_{x,g/P} \quad (2)$$

$\vec{a}_{x,g}$ is the vector from point P to a point on the x axis, as illustrated in Figure 2. $\vec{a}_{x,g/P}$ is the vector from the centre of gravity c_g to point P, as illustrated in Figure 2. F_pH acts on the wheels in the horizontal direction. The wheels translate this force into a torque τ_w. Reversibly the torque generated by the motor will act on the body angle Θ_p. More detailed
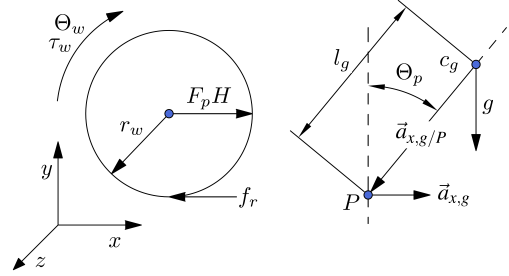

Fig. 2.   Wheel and robot body free body diagrams.

information about the linear model can be found in [3].

B. Parameter Identification

Some of the parameters are directly measurable. The dynamic friction coefficient estimation is described in the following, as it is specific for this work. All relevant system parameters are listed in the nomenclature . The test is done by making the robot free-fall, without holding the wheels, while recording the angular velocity with a gyroscope, the results are shown in Figure 3. A second test is done, similar to the initial test, except this time the wheels of the robot are kept still in one place. The acceleration of the two tests is subtracted, which enables the isolation of the negative acceleration. From here the frictional coefficient of the motor shaft can be calculated.
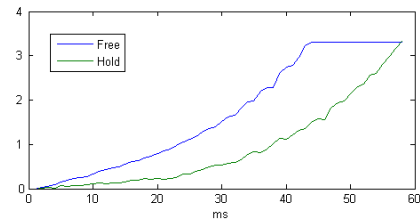

Fig. 3.   Friction experiment: Acceleration of the free-falling robot, tightened and loose wheels

C. Linear Model Validation

A comparison of the simulated model response with an experimental response is shown in Figure 4.
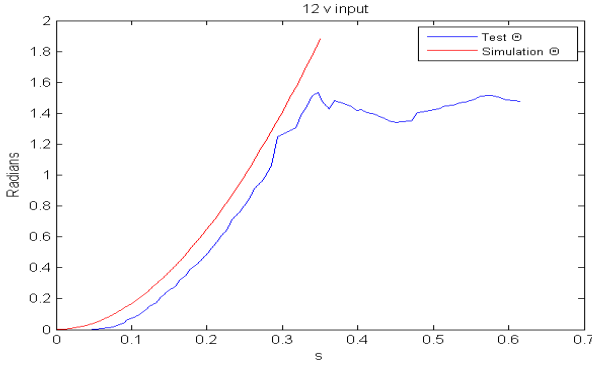

Fig. 4. Validation of the linear model.

The validation result of the model is good, the model matches the experimental data within 1.2 radians. Except for the delay which occurs from 0 to 50 ms. We believe this is partly due to the backlash influence, which immobilizes the platform until the backlash gap has been crossed Thereby, in the following, we dedicate our work to model the backlash effect and try to prevent its influence.

D. Non-Linear Model

When the system operation enters backlash mode, the free gap will make the torque transfer from the motor to the load disappear until the free gap vanishes. This influence is illustrated in Figure 5.

The model of the backlash can be introduced as an exact model, also referred to as the sandwich model [5], [6]. The free body diagram shown in Figure 6 represents the sandwich model [5], where the gearing backlash could be modeled as a non-linear relationship between the load torque T_l and shaft torque T_s.
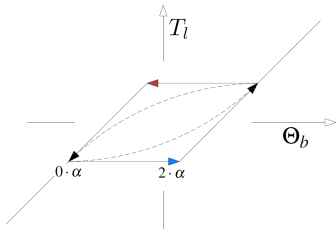

Fig. 5. Effect of backlash where the torque transfer is interrupted from $0 \cdot \alpha$ to $2 \cdot \alpha$.
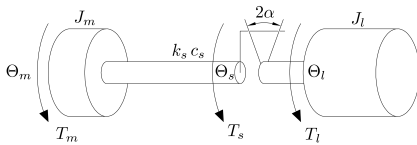

Fig. 6. Illustration of the sandwich model, where the backlash gap is present between the motor and the load.

Another kind of backlash model is called the exact model which describes all aspects of the backlash, as well as the elasticity of the shaft in the gearing.

According to Figure 6, the motor kinetic dynamics can be described as:

$$J_m \ddot{\Theta}_m = -c_m \dot{\Theta}_m - T_s + T_m \qquad (3)$$

The load part dynamics can be described as:

$$J_l \ddot{\Theta}_l = -c_l \dot{\Theta}_l + T_s - T_d \qquad (4)$$

Furthermore,

$$\dot{\Theta}_d = \dot{\Theta}_m - \dot{\Theta}_l \qquad (5)$$

The transmitted shaft torque is described as following;

$$T_s = k_s \Theta_d + c_s \dot{\Theta}_d \qquad (6)$$

The backlash angle is represented as the difference angle $\dot{\Theta}_b \hat{=} \dot{\Theta}_d - \dot{\Theta}_s$. The backlash angle dynamics are described as:

$$\dot{\Theta}_b = \begin{cases} max\left(0, \dot{\Theta}_d + \frac{k_s}{c_s}(\Theta_d - \Theta_b)\right) & if \quad \Theta_b = -\alpha, \\ \dot{\Theta}_d + \frac{k_s}{c_s}(\Theta_d - \Theta_b) & if \quad |\Theta_b| < \alpha, \\ min\left(0, \dot{\Theta}_d + \frac{k_s}{c_s}(\Theta_d - \Theta_b)\right) & if \quad \Theta_b = \alpha \end{cases} \qquad (7)$$

For more information on the exact model, we refer to [5], [6], [7], [8], [9].

The third type of backlash model is a simplification of the exact model. The hysteresis model assumes that the shaft is stiff which eliminates k_s and c_s. This model requires an assumption that the load disturbance is 0 and that the friction in the backlash gap is 0. This means that the load moves with constant velocity, under the assumption that friction is ignored, in the backlash gap.

$$\begin{cases} \dot{\Theta}_l(t) = \dot{\Theta}_m(t) & if \quad \dot{\Theta}_m(t) > 0 \quad and \quad \Theta_l(t) = \Theta_m - \alpha \\ \dot{\Theta}_l(t) = \dot{\Theta}_m(t) & if \quad \dot{\Theta}_m(t) < 0 \quad and \quad \Theta_l(t) = \Theta_m + \alpha \\ \ddot{\Theta}_l(t) = 0 & elsewhere \end{cases} \qquad (8)$$

This work will concentrate on the hysteresis model.

IV. CONTROL DESIGN

A. linear control

This controller is used when the system operates within the normal mode, i.e., the situation where the backlash is not present in the system operation. This controller is designed according to the LQR solution.

B. Proportional Backlash Controller

This controller is purposely designed for the backlash mode, i.e., when the backlash is present in the system operation. The proportional backlash controller uses the backlash angle as a feedback input, and it outputs the control signal to the motors accordingly:

$$u(t) = K_p \cdot \Theta_b(t) \qquad (9)$$

Where Θ_b represents the backlash angle, and the proportional constant K_p is determined according to:

$$K_p = u_{max}/\Theta_{b_{max}} \qquad (10)$$

The effect of this type of controller is that the motors have more power at the beginning when the backlash effect happens, and decrease as the backlash angle becomes smaller. It ensures a good compromise between speed and gentility.

C. Switching Control

This non-linear controller is designed based on the hysteresis model, described by Equation 8. Hereby this controller is a type of hybrid controller, which switches between the linear controller and the Backlash controller. It is assumed that direction change, sets the system in backlash mode until the backlash angle is crossed, this is illustrated in Figure 7. When the switch goes into backlash mode the proportional backlash controller is activated.
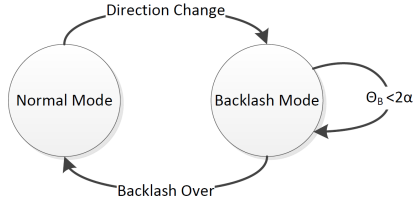

Fig. 7. The hybrid switching controller.

D. Backlash Detection

The backlash is detected based on the velocity change of the platform, as when the system changes velocity it will go from contact mode into backlash mode. Estimation of the backlash angle is done by measuring the motor position and subtracting it from the maximal backlash angle, which is a constant (2α).

E. Weighting of the Switching Controller

During tests of the system, we observed that the developed switching controller proved to decrease the power of the linear controller at larger body tilt angles, where the backlash controller was activated due to minor changes in direction, and it thus interrupted the linear controller from stabilizing the platform [3]. Thereby switching controller weighing, according to different tilt body angle, is introduced to reduce the activity of the backlash controller at larger angles, this idea is illustrated in Figure 8. The weighting of the backlash controller as a
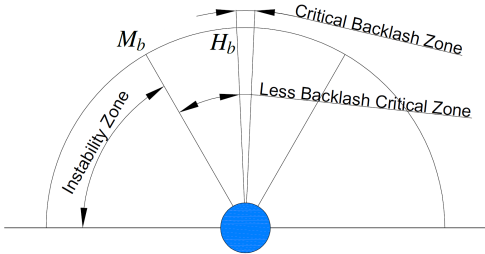

Fig. 8. Weighting regions of the backlash based on the tilt angle.

function of the tilt body angle is described as:

$$\dot{\Theta}_1(t) = \begin{cases} C_b = 0 & if & \Theta_p > M_b \\ C_b = f(\Theta_p) & if & M_b > \Theta_p > H_b \\ C_b = 2\alpha & elsewhere \end{cases} \qquad (11)$$

The critical angles H_b and M_b are determined through trial and error based on experience with the system [3]; where $H_b = 0.17$ *rad* and $M_b = 0.6$ *rad*.

V. TESTS AND RESULTS

One of the LQR Controller Tests:: Plot in Figure 9 represent the robot body tilt angle and corresponding angular velocity. A FFT plot is presented in Figure 10, which identifies the amplitude of the signals without the backlash controller. The results in Figure 9 indicate violent oscillations of the
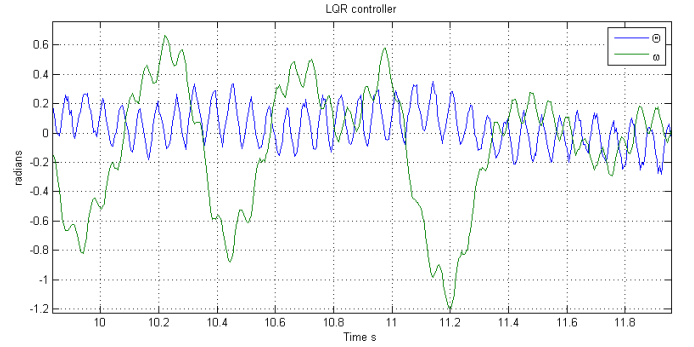

Fig. 9. Performance due to a standard LQR controller developed based on the linear model.
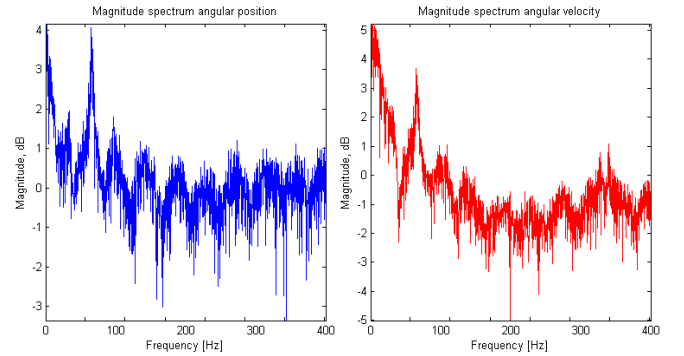

Fig. 10. FFT plots of the angle and angular velocity data due to the LQR controller.

angular position and velocity, and the FFT in Figure 10 reveals a spike in the frequency around 35 Hz, which indicates the robot system's structural resonance frequency.

One of the Switching Controller Tests:: The use of the proportional backlash controller dramatically reduces the oscillations as can be seen in Figure 11. The angular position in the test without the switching controller, oscillates with a peak-to-peak angle of up to 0.4 rad, while with the switching controller it is reduced to 0.2 rad. The reduction is greatest while the system is close to equilibrium point. The FFT plots due to the switching controller can be seen in Figure 12, which reveals an oscillation reduction of 2 dB, or a halving at system's resonance frequency. The damping occurs with
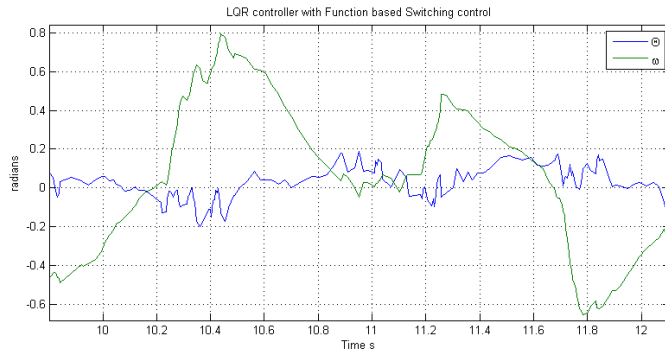
Fig. 11. Performance due to the developed switching controller (between LQR and Proportional backlash control).
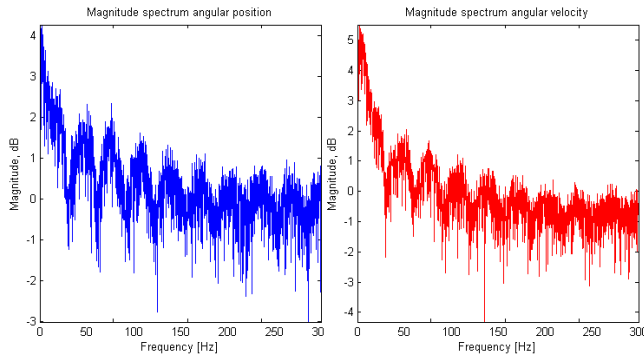

Fig. 12. FFT plots of the angle and angular velocity data due to the switching control.

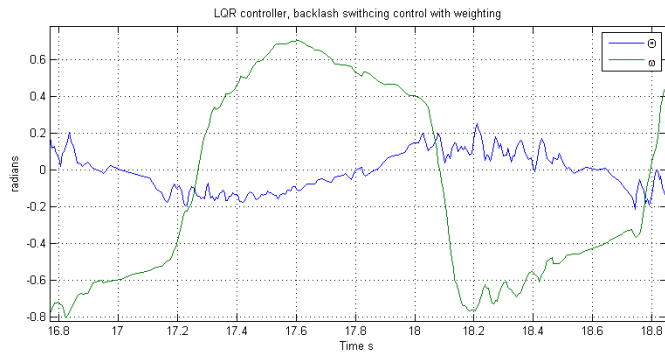similar intensity both for the angular velocity and angular position.

Fig. 13. Performance due to switching control with weighting function.

The Switching Controller with Added Weighting: The weighting function helps smoothen the systems performance further, as illustrated in Figure 13, and the controller is more active when the tilt angle is further away from the equilibrium point.

Long Time Interval Comparison: The long time interval tests illustrate how the platform behaves over a longer period of time, refer to Figure 14 and 15, respectively for the LQR and the switching controller. These two controllers illustrate how the switching controller reduces the noise in the signal, notice that the angle reaches almost 1 rad multiple times, proving
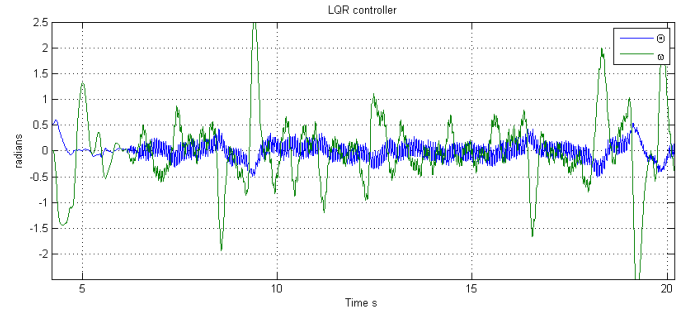

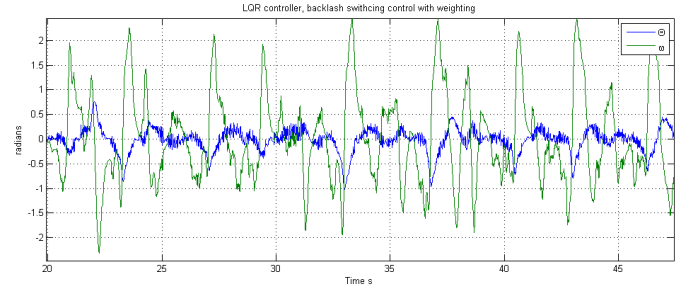Fig. 14. Performance due to LQR long time interval.

Fig. 15. Performance due to switching controller long interval.

system instability. This is caused by a faulty platform design, incapacitating the motors from successfully achieving system stability, later work involved a new and improved platform.

PID: In order to make further comparison with a typical control solution, a PID was designed for the considered robot system. The result of the PID controller is displayed in Figure 19. It is clearly observed that the result of the PID controller is similar to that of the LQR controller, the test exhibits a lot of oscillations around 35 Hz. This is mainly due to the backlash effect, which is similar to the LQR controller case.
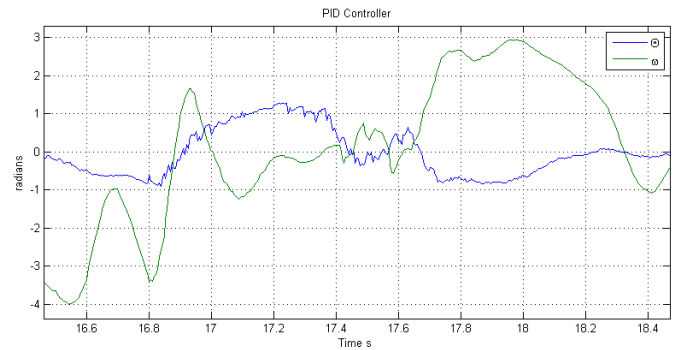

Fig. 16. Performance due to the PID controller.

Tests Made on the Improved Platform: Tests with the new platform are presented in Figure 17, 18 and 19, respectively for the LQR controller, the switching controller and the benchmark PID controller.

In the tests with the improved platform; stability was achieved with all three controllers, and the switching controller proved once again to reduce the noise created by the backlash. We have experienced that using the switching controller
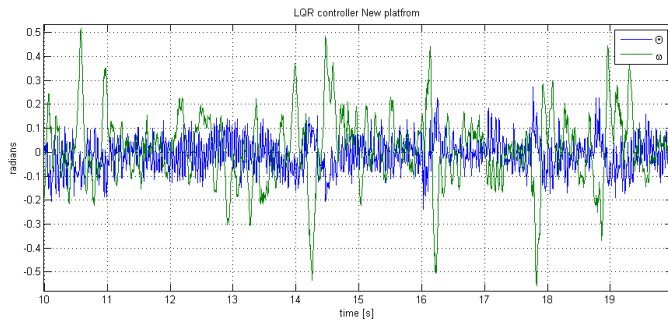
Fig. 17. Tests made with the updated platform: Performance due to LQR controller, 10 second interval.
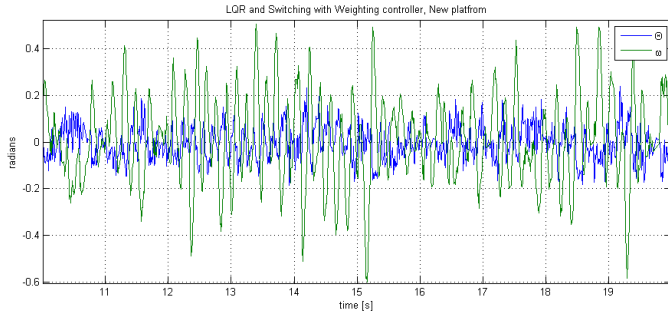

Fig. 18. Tests made with the updated platform: Performance due to LQR with switching controller, 10 second interval.

without the weight increased the probability of the system becoming unstable. Adding the weight increased the power of the controller at higher angles, which resulted in a smoother performance.

VI. CONCLUSION

The goal of this work is to apply a simple switching controller solution (sliding mode controller) for stabilizing an open-loop unstable self-balancing robot system with a heavy backlash feature. The backlash effect in the considered system is mainly due to a gear transmission part. The backlash effect can be clearly observed when a standard linear controller is employed. The robot tilt angle and angular velocity exhibit large oscillations, especially when the system approaches the balancing position. The switching controller provides a smoother performance. It switches the controller law between
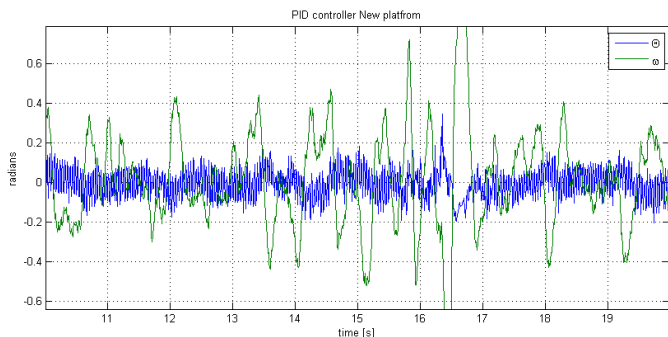

Fig. 19. Tests made with the updated platform: Performance due to PID controller, 10 second interval.

a normal and backlash mode, where the backlash mode controller is a P-type controller with respect to the backlash angle and the normal mode controller is a LQR solution. The detection of the backlash phenomenon occurrence and the backlash angle estimation are also discussed.

The best performance is achieved with a switching controller using a weightings function to the backlash controller which is predetermined according to critical body tilt angles. The implementation and extensive tests show that the developed control solutions can be easily adopted. Furthermore it is a simple, and very effective way of handling the backlash affected control systems. Stability was not achieved with the initial platform due to a faulty design, but an improved platform proved stable and the switching controller using a weightings function once again proved its superiority over the LQR and PID controller.

REFERENCES

[1] Dan Simon, Optimal State Estimation: Kalman, H Infinity, and Nonlinear Approaches, John Wiley & Sons, 2006, 1th Edition, 0-471-70858-5

[2] Gang Tao and Petar V Kokotovic, Adaptive Control of Systems with Actuator and Sensor Nonlinearities, Wiley Inter-Science, 1996, 1th Edition, 0-471-15654-3

[3] Petar Durdevic, Balancing Robot, 6-6-2011, Project report, Aalborg University Esbjerg

[4] R M R Bruns and J F P B Diepstraten and X G P Schuurbiers and J A G Wouters, Motion Control of Systems with Backlash, 29/8-2006, Eindhoven Technische Universiteit Eindhoven

[5] Mattias Nordin and Per Olof Gutman, Controlling mechanical systems with backlash a survey, Automatica 38, pp. 1633-1649, 2002, Eindhoven Technische Universiteit Eindhoven

[6] Adam Lagerberg, A literature Survey on Control of Automotive Power-trains With Backlash, Control and automation laboratory, pp. 1-15, 2001, Chalmers University of Technology, Goeteborg, Sweden

[7] Adam Lagerberg and Bo S Egardt, Backlash Gap Position Estimation In Automotive Powertrains, European Control Conference ECC 03, September 1-4, 2003, Cambridge, UK

[8] Adam Lagerberg and Bo S Egardt, Estimation of Backlash With Application to Automotive Powertrains, Decision and Control, 2003 Proceedings 42nd IEEE Conference, pp. 4521 - 4526, Vol 5, 9-12 Dec 2003, Maui HI, USA, 0-7803-7924-1

[9] Odai M and Hori Y, Speed control of 2-inertia system with gear backlash using gear torque compensator, Advanced Motion Control, pp. 234 - 239, 29 Jun-1 Jul 1998, Sweden

[10] Dan Simon, Kalman Filtering, Embedded Systems Programming, pp. 72-79, Cleveland State University, USA, June 2001

[11] Bernard Friedland and Lady Davis, Feedback control of systems with parasitic effects, Proceedings of the American Control Conference, Series D, pp. 937-941, Albuquerque, New Mexico, June1997

[12] Mattias Nordin and Per-Olof Gutman, Non-Linear Speed Control of Elastic Systems with Backlash, Proceedings of the 39th IEEE, pp. 4060-4065, Sydney, Australia, December 2000

[13] Raymond de Callafon and Gabe Graham, Desperately Seeking Sensor, IEEE Control System Magazine Feb 2011 , pp. 16-17 IEEE, Piscataway, NJ 08854, USA

[14] M. L. Corradini and G. Orlando and G. Parlangeli , Robust control of nonlinear uncertain systems with sandwiched backlash, 44th IEEE Conference on Decision and Control, and the European Control Conference 2005 , pp. 8112-8117, Seville, Spain, December 12-15, 2005